HHS Public Access

Author manuscript

Cancer Discov. Author manuscript; available in PMC 2015 November 01.

Published in final edited form as:

Cancer Discov. 2015 May ; 5(5): 520–533. doi:10.1158/2159-8290.CD-14-1101.

Intratumoral heterogeneity in a p53 null mouse model of human breast cancer

Mei Zhang[a,1], **Anna Tsimelzon**[b], **Chi-Hsuan Chang**[c], **Cheng Fan**[d], **Andrew Wolff**[a], **Charles M. Perou**[d,e], **Susan G. Hilsenbeck**[b], and **Jeffrey M. Rosen**[c,1]

[a]Department of Developmental Biology, University of Pittsburgh, 204 Craft Ave., Pittsburgh, PA, 15213, USA

[b]Lester & Sue Smith Breast Center, One Baylor Plaza, Houston, TX 77030, USA

[c]Department of Molecular and Cellular Biology, Baylor College of Medicine, One Baylor Plaza, Houston, TX 77030, USA

[d]Lineberger Comprehensive Cancer Center, University of North Carolina, Chapel Hill, 27599, USA

[e]Departments of Genetics, and Pathology & Laboratory Medicine, University of North Carolina, Chapel Hill, 27599, USA

Abstract

Intratumoral heterogeneity correlates with clinical outcome and reflects the cellular complexity and dynamics within a tumor. Such heterogeneity is thought to contribute to radio- and chemoresistance since many treatments may only target certain tumor cell subpopulations. A better understanding of the functional interactions between various subpopulations of cells, therefore, may help in the development of effective cancer treatments. We identified a unique subpopulation of tumor cells expressing mesenchymal-like markers in a p53 null mouse model of basal-like breast cancer using fluorescence-activated cell sorting and microarray analysis. Both in vitro and in vivo experiments revealed the existence of crosstalk between these “mesenchymal-like” cells and tumor-initiating cells. Knockdown of genes encoding ligands upregulated in the mesenchymal cells and their corresponding receptors in the tumor-initiating cells resulted in reduced tumorigenicity and increased tumor latency. These studies illustrate the non-cell autonomous properties and importance of cooperativity between tumor subpopulations.

Keywords

intratumoral heterogeneity; tumor-initiating cells; cancer stem cells; niche cells; signaling pathway; cell; cell interaction

[1]To whom correspondence should be addressed. Mei Zhang, Department of Developmental Biology, 204 Craft Ave., Pittsburgh, PA, 15213, USA; Telephone: 412-641-7726; Fax: 412-641-2458; meizhang@pitt.edu. Jeffrey M. Rosen, Department of Molecular and Cellular Biology, One Baylor Plaza, Houston, TX 77030, USA; Telephone: 713-798-6210; Fax: 713-798-8012; jrosen@bcm.edu.

Conflict of Interest Statement: The authors disclose no potential conflicts of interest.

Introduction

Cell–cell interactions, through paracrine signaling, play critical roles in the regulation of mammary morphogenesis. While most of these interactions involve luminal to basal signaling (1), a recent study has shown that basal cells may regulate luminal progenitor activity during pregnancy and lactation processes through p63-neuregulin signaling (2). Similarly, tumorigenesis is a multistep process involving acquired genetic and epigenetic alterations that generate individual cell populations with aberrant differentiation and proliferation potential. Intratumoral heterogeneity (ITH) has been considered one important factor in assessing a patient's initial response to treatment and selecting drug regimens to effectively increase tumor response rates (3, 4). Understanding the molecular interactions between various subpopulations of tumor cells, as well as their interaction with the microenvironment, may provide new targets for treatment to help in eradicating both primary and recurrent tumors. Most studies have focused to date on the latter, i.e. the interactions of tumor cells with the microenvironment, e.g. tumor-associated fibroblasts, macrophages, endothelial cells, osteoblasts, etc. However, little is known about the importance of possible tumor cell-tumor cell and paracrine interactions that may be important within the intrinsic tumor cell population.

ITH has long been recognized from a pathological point of view (5) and has been identified at the molecular level in the past few years through large scale transcriptome and genome analyses (6, 7). ITH is thought to be generated through subclonal evolution during tumor progression (8), with different clones displaying various capabilities of tumor propagation and responses to therapy (8–12). Such variability within a tumor may be partially explained by the cancer stem cell (CSC) theory. Contrary to the monoclonal theory of cancer (5), the CSC theory has suggested that a subpopulation of CSCs (a.k.a. tumor-initiating cells, TICs) can self-renew and differentiate along a particular lineage to generate the bulk of tumor "non-stem" cells (7). Using a strategy of transplanting fluorescence-activated cell sorting (FACS) sorted single cells from solid tumors into immunodeficient mice, a small subpopulation of TICs has been identified from a variety of solid tumors including breast (13). The ability to form secondary mammospheres after plating the cells dissociated from primary spheres cultured on a non-adherent substratum also has been utilized as a surrogate for an in vivo stem cell self-renewal assay (14). The mammosphere and stem cell subpopulations have been shown to be more resistant to chemotherapy and radiation treatment as compared with the total cells and non-stem cells, respectively (15–17). This has been hypothesized to result in cancer recurrence and metastasis after the initial treatment.

While the CSC theory may apply in many subtypes of cancers, including breast cancer, increasing evidence has suggested non-TICs, although less tumorigenic than the TICs, may generate aggressive TICs within a tumor (18). Li and Clevers (19) have proposed a theory of co-existence of both active and quiescent stem cells in several tissues as both cycling yet long-lived populations of stem cells have been identified. However, "gold standard" limiting dilution transplantation assays most commonly used in the characterization of stem cells from various tissues, might only identify active (cancer) stem cells. Therefore, investigation of ITH will provide important insights into the roles of stem cells as well as their interactions with other tumor cells in tumor initiation, progression, and treatment resistance.

Our previous studies defined a Lin^{-}CD29 (β1 integrin)$^{High(H)}$CD24^{H} subpopulation of TICs by both limiting dilution transplantation and *in vitro* mammosphere assays using a syngeneic p53 null mouse mammary tumor model (20). Using FACS and microarray analysis, these studies also identified a unique group of cells in these tumors expressing "mesenchymal-like" cell markers. Factors such as cytokines, chemokines, growth factors and secretory Wnt proteins that have been reported to function as niche components in various tissues, were significantly increased within the mesenchymal-like tumor cell subpopulation. The stem cell niches characterized to date in the mouse use Wnt signaling, Notch signaling, IL6, or CXCL12 to regulate stem cell function (21). All these factors are important autocrine or paracrine cues that affect diverse processes in normal tissue development and tumorigenesis. The functional interaction between niche cells and TICs, therefore, were investigated by comparing the properties of the combined "mesenchymal-like" and TIC subpopulations to the individual isolated subpopulations alone. Co- and transwell-cultures of putative niche cells with TICs in serum-free suspension mammosphere assays revealed that both the *in vitro* self-renewal ability and the proliferation potential of the TICs were enhanced in the presence of the niche cells or factors secreted from the niche cells. *In vivo* co-transplantation assays indicated that the niche cells enhanced the TIC tumor initiation potential when a limited number of TICs was present. Transduction of niche cells with lentiviral expressed short hairpin RNAs (shRNAs) directed against Wingless-type MMTV integration site family, member 2 (Wnt2) and Cxcl12 ligands differentially expressed within the niche population, resulted in reduced mammosphere frequency and decreased in vivo tumorigenic potential with increased latency. Knockdown of the receptors for these ligands in the TIC subpopulation also provided additional evidence of the importance of functional interactions between these tumor subpopulations.

Results

A Lin^{-}CD29^{H}CD24$^{Low(L)}$ subpopulation from p53 null mammary tumors displays a mesenchymal-like gene expression profile

Cell surface markers CD29 and CD24 separated dissociated p53 null tumor cells into four subpopulations: CD29^{H}CD24^{H}, CD29^{H}CD4^{L}, CD29^{L}CD24^{H}, and CD29^{L}CD24^{L}. The lineage (Lin)$^{-}$CD29^{H}CD24^{H} subpopulation displayed a significantly increased tumorigenic potential as compared to the other subpopulations (20). PCR genotyping performed using p53 primers (X7/X6.5 defining p53 wild-type, and X7/NEO19 defining p53 null) confirmed the p53 null status of all the individual subpopulations suggesting their non-host cell of origin when 30-cycle of PCR was performed (Supplementary Figure S1A, left). A small trace of p53 wild type product was detected when a 35-cycle of PCR was performed most likely due to infiltrating immune cells within the tumors (Supplementary Figure S1A, right).

To determine whether there exist genomic copy-number differences among the four subpopulations, we performed high resolution mouse whole-genome bacterial artificial chromosome (BAC)-based comparative genomic hybridization (CGH) array which covers the entire mouse genome (22, 23). The syngeneic Balb/c mouse tail DNA was used as control. The chromosomal copy-number profiles performed on the four subpopulations of the p53 null tumor did not show significant variations (Supplementary Figure S1B).

We have previously shown that the $Lin^{-}CD29^{H}CD24^{L}$ subpopulation identified in most of the heterogeneous p53 null tumors studied (including estrogen receptor positive $(ER)^{+}$ and negative (ER^{-}) tumors, tumors expressing basal/myoepithelial markers K5/K14, as well as those only expressing luminal marker K8), was usually <5% of the total cell population. The TIC subpopulation (i.e. $Lin^{-}CD29^{H}CD24^{H}$) was able to generate tumors with as few as 10 cells. The $Lin^{-}CD29^{H}CD24^{L}$ subpopulation was also able to generate tumors, but only when more cells were transplanted indicating a reduced tumorigenic potential as compared to the TIC population (20). Nevertheless, such cells displayed increased tumorigenicity when compared with the $Lin^{-}CD29^{L}CD24^{H}$ and $Lin^{-}CD29^{L}CD24^{L}$ subpopulations which represented the bulk (>90%) of the tumor cells. However, FACS analysis of tumors arising from the $Lin^{-}CD29^{H}CD24^{L}$ showed that they did not mimic the phenotype of the parental tumor, instead, an expansion of the TICs was observed from the $Lin^{-}CD29^{H}CD24^{L}$-derived tumors (Supplementary Figure S2A and (20)). TIC-derived tumors, like the primary tumors (Supplementary Figure S2Ba), express SMA mainly in the ductal structures (Supplementary Figure S2Bb), however, a high level of SMA also was observed in the stromal compartment in the $CD29^{H}CD24^{L}$ derived tumors (Supplementary Figure S2Bc).

Microarray analysis (described in details in the Supplementary Information (SI) and reported previously (20)) to compare the expression of the $CD29^{H}CD24^{L}$ cells with those of the other three subpopulations identified an increased expression of Wnt proteins, including Wnt ligands Wnt2, Wnt9a, and Cxcl12 and Il6 in this subpopulation (Supplementary Table S1). Interestingly, the TICs in the p53 null tumor T1, a squamous adenocarcinoma expressed a higher level of both Axin2 and Tcf7, both of which are known targets of Wnt signaling as demonstrated by qPCR (Figure 1A & 1B), suggesting the possible interaction between the TICs and the $CD29^{H}CD24^{L}$ cells. The expression of Fzd7, one of the Wnt ligand receptors, and Cxcr4, the receptor for CXCL12 was also upregulated in the TIC population as compared with the non-TIC population (Figure 1C & 1D).

$CD29^{H}CD24^{L}$ subpopulation is less proliferative compared with the TIC population

Cell cycle analysis performed on TICs and $CD29^{H}CD24^{L}$ cells using 7-AAD and pyronin Y and showed that 8.6±1.3% (mean±SD) of TICs were in G0/G1 phase (Figure 2Aa), while 21.5±3.3% of $CD29^{H}CD24^{L}$ were in the G0/G1 phase (Figure 2Ab). A more detailed characterization of the 20% cells in the G0/G1 phase showed that 17.4±3.7% of the $CD29^{H}CD24^{L}$ cells were in the G0 phase and 3.2±0.3% in the G1 phase (Figure 2Ba&b), indicating that a group of $CD29^{H}CD24^{L}$ cells were quiescent. However, this cannot explain the low tumorigenic potential of this subpopulation as the $CD29^{H}CD24^{L}$ cells contain more cells in the G0 phase, and have a higher tumorigenic potential than the $CD29^{L}CD24^{H}$ (Supplementary Figure S3A, G0/G1: 9.6±2.1%; Supplementary Figure S3B, G0: 7.8±1.9%), and $CD29^{L}CD24^{L}$ cells (Supplementary Figure S3C, G0/G1: 12.6±1.9%; Supplementary Figure S3D: G0: 8.9±1.6%), respectively. We further measured the proliferative potential of the individual populations after FACS and cytospin centrifugation followed by Ki67staining. While 60% of TICs (Figure 2Ca) were proliferative, only 30% of $CD29^{H}CD24^{L}$ (Figure 2Cb) cells were Ki67 positive (Figure 2D).

$CD29^{H}CD24^{L}$ niche population has features of mesenchymal and claudin-low

Since several genes expressed in the $CD29^{H}CD24^{L}$ niche population have been associated with cells undergoing an epithelial to mesenchymal (EMT) transition, we performed a comprehensive analysis of the RNA expression profiles of the individual populations using previously identified mesenchymal (24), and claudin-low gene signatures (25, 26). This analysis strongly supports the observation that the $CD29^{H}CD24^{L}$ population expresses mesenchymal markers (Figure 2Ea). The mesenchymal gene expression signature was highly correlated with the claudin-low tumor subtype, with the claudin-low subtype defining signature showing high expression in the $CD29^{H}CD24^{L}$ subpopulation that also displays an increased expression of EMT features (Figure 2Eb&2Ec).

$CD29^{H}CD24^{L}$ promotes in vitro self-renewal capacity of TICs

Co-culture of $CD29^{H}CD24^{L}$ cells (labeled with red fluorescent cell linker dye, PKH 26) with TICs (labeled with green fluorescent cell linker dye, PKH 67) in serum-free mammosphere assays generated both larger and an increased number of mammospheres as compared with culturing the TICs or $CD29^{H}CD24^{L}$ cells alone (Figure 3A & 3B). However, the co-culture of TIC and $CD29^{L}$ cells did not result in increased mammosphere frequency indicating the unique interaction between the TIC and $CD29^{H}CD24^{L}$ cells (Figure 3B). These results suggest that both the in vitro self-renewal ability and proliferation potential of the TICs are enhanced in the presence of the niche cells. To directly test this hypothesis, the levels of CXCL12 expression under different culture conditions were measured (Supplementary Figure S4). The levels of CXCL12 secreted by $CD29^{H}CD24^{L}$ cells, either cultured alone or together with TICs, were significantly higher than observed with TICs alone, indicating that CXCL12 is both regulated and functioning via a paracrine mechanism to promote the in vitro self-renewal ability of TICs.

Next, we used a transwell assay to determine whether direct cell–cell contact or secreted factors are required to enhance the self-renewal potential of TICs when cultured under the serum-free condition. A 0.4 μm filter was employed to prevent the passage of both cell types through the membrane. Under these conditions, TICs cultured with the putative niche cells resulted in an increased number (Figure 3C), but not size of mammospheres as compared with that of the TICs with themselves. A marginal significantly (**p=0.051) higher mammosphere forming efficiency of TICs was observed in the presence of niche cells alone as compared to that in the presence of TIC and niche cells. This result suggests that soluble factors secreted from the putative niche cells support the self-renewal of TICs, but possibly not their proliferation. When TICs, after transwell-culture with or without $CD29^{H}CD24^{L}$ cells, were transferred to Growth Factor Reduced Matrigel, branching structures were observed if the TICs were previously transwell-cultured with the putative niche cells, while no branching structures were observed if they were transwell-cultured with the TICs alone (Figure 3D), suggesting the secreted molecules from the niche cells were able to affect the differentiation potential of the TICs.

Downregulation of preferentially expressed genes in the putative niche cells ($CD29^{H}CD24^{L}$) inhibited the self-renewal of TICs

We next determined the functional role of secreted factors previously identified by our microarray studies. Since Wnt signaling and CXCL12 secretion are known to increase the self-renewal potential of TICs (27–29), we hypothesized that repression of Wnt2 and Cxcl12 expression in the niche cells alone might be inhibitory. FACS sorted $CD29^{H}CD24^{H}$ TICs have increased expression of Fzd7, Tcf7 and Axin2, components of the Wnt signaling pathway as compared with the non-TICs (Figure 1). This finding is consistent with the previous studies showing the TIC subpopulation identified using cell surface markers (CD29 and CD24) overlapped with active canonical Wnt signaling cells identified using a Wnt reporter system (17). We thus performed co-culture experiments using different combinations of Wnt reporter-marked TOP-GFP^{+} TICs, and niche cells with Wnt2 shRNA knockdown. $CD29^{H}CD24^{H}$ TICs were used to co-culture with the niche cells with Cxcl12 shRNA knockdown.

FACS sorted $CD29^{H}CD24^{L}$ niche cells were transduced with a lentivirus expressing two different shRNAs to knock down expression of either Wnt2 or Cxcl12 differentially expressed in the niche population. Two clones targeting Wnt2 and one targeting Cxcl12, and their corresponding non-silencing controls were included. Real-time qPCR confirmed the down-regulation of Wnt2 and Cxcl12 in the p53 null T1 tumor at levels ranging from 50 to 60% (Figure 4A & 4B). Genetically modified knockdown niche cells were then co-cultured with TICs in serum-free mammosphere medium under non-adherent conditions for 7 days. A reduced mammosphere forming ability was observed for both knockdowns, indicating that the functional interaction between two cell types was disrupted, and the self-renewal potential of the TICs was inhibited (Figure 4C & 4D).

Downregulation of Fzd7 and Cxcr4 in the TICs ($CD29^{H}CD24^{H}$) in combination with downregulation of Wnt2 and Cxcl12 in the niche cells significantly inhibited the in vitro self-renewal of TICs

A higher expression of Fzd7 in the Wnt responsive TIC population as compared to the non-TIC population has suggested that Fzd7 may play a role in the interaction of TIC with the surrounding cells through Wnt signaling. To determine the functional interaction between TICs and niche cells, Fzd7 and Cxcr4, Wnt2 and Cxcl12, were knocked-down, respectively, in the TIC and niche population, and their in vitro self-renewal potential were analyzed using mammosphere assays. Both Fzd7 and Cxcr4 expression were decreased by 75% and 55%, respectively, in the TICs as confirmed by qRT-PCR (Figure 4E & 4F). When genetically modified TICs and niche cells were co-cultured, a significant decrease of the mammosphere forming ability was detected in both knockdowns, with the co-culture of the knockdown in both TIC and niche population exhibiting a greater reduction of mammosphere forming ability as compare with the ligand knockdown alone (Figure 4G & 4H). In addition, when Il6 was knocked-down in the niche cells (Supplementary Figure S5A), and such modified niche cells were co-cultured with TICs, a decrease mammosphere forming efficiency was observed (Supplementary Figure S5B).

$CD29^{H}CD24^{L}$ niche cells enhanced TICs tumor initiation potential shown by limiting dilution co-transplantation assay

These in vitro assays were suggestive of a functional interaction between the TICs and niche cells. This was confirmed using an in vivo limiting dilution analysis. Transplantation of 10 $CD29^{H}CD24^{L}$ niche cells alone did not initiate tumor formation, while in contrast at least 10 TICs were capable of initiating tumor formation (Table 1A and Supplementary Table S2). However, transplantation of 2 TICs, with a tumor formation frequency of 2 of 8, was able to initiate tumorigenesis when co-transplanted with 10 niche cells. Co-transplantation of increasing numbers of niche cells resulted in increasing numbers of tumors (Supplementary Table S3 and Figure 5A). This limiting dilution analysis involving several doses of TICs, revealed significant differences between groups defined by the numbers of niche cells: Chisq 10.1753 on 2 degrees of freedom (DF), p-value=0.006. Co-injection of 10 niche cells vs 0 niche cells showed a 4.7-fold increase in tumor formation (p=0.0017), while the effect of co-injection of 2 niche cells was intermediate (about 3-fold) and not clearly different from either 10 or 0 niche cells (co-injection of 0 niche cells vs. 2 niche cells: p-value=0.09372; 2 niche cells vs. 10 niche cells: p-value=0.0523). These results suggest that the "mesenchymal-like" niche cells ($CD29^{H}CD24^{L}$) were able to enhance TIC tumor initiation by secreting factors that perhaps provide an improved microenvironment.

The time to tumor formation curves were also estimated and compared (Figure 5B). Across all 8 groups, there was a significant difference between groups ($p<0.001$). Two groups (TICs=0/Niche=10 and TICs=5/Niche=0) did not have any tumors, but differences remained significant even after eliminating these 2 groups (P=0.002). For fixed numbers of niche cells (i.e. niche cells=10), tumor latency was decreased with increasing numbers of TICs (Supplementary Table S4a). In order to investigate whether niche cells reduced the time to tumor formation, two sets of comparisons were undertaken. With 10 TICs, tumor formation was more rapid with 10 niche cells as compared to 0 (p=0.02, Supplementary Table S4b), while 2 niche cells was not different from either 0 or 10. Finally, with 20 TICs, tumor formation was faster with 10 niche cells as compared to 0 (p=0.02, Supplementary Table S4c).

Co-transplantation of the fluorescence labeled TICs (pEIT-TICs) and $CD29^{H}CD24^{L}$ niche cells (pEIZ-niche cells) suggested that the TICs contributed to the majority of tumor growth

TICs and putative niche cells ($CD29^{H}CD24^{L}$) were individually infected with the lentiviral expression system ZsGreen and Tomato red, and were individually or separately co-transplanted into the 3-wk-old cleared fat pad recipient mice. FACS analysis demonstrated that majority of the resulting tumor cells were derived from the TICs when TICs and niche cells were mixed at different combinations of 200/0 (Supplementary Figure S6Ba&b); 120/80 (Supplementary Figure S6Bc&d); 68/132 (Supplementary Figure S6Be&f); and 32/168 (Supplementary Figure S6g&h), consistent with their self-renewal and differentiation ability.

Downregulation of Wnt2 in the niche cells ($CD29^{H}CD24^{L}$) inhibited the in vivo self-renewal of TICs through limiting dilution transplantation assay

To determine if the in vivo tumor initiating ability of TICs was affected when secreting factors were repressed, we also co-transplanted the genetically modified (shRNA knocked-down of Wnt2) niche cells, together with the TICs (Wnt-responsive cells), into the cleared fat pads of recipient mice. A decreased tumorigenic potential and a longer latency were observed with different combinations of TOP-GFP transduced GFP^{+} TICs and Wnt2 shRNA knockdown niche cells as compared with those of co-transplantation of TICs and control niche cells, suggesting the tumorigenic potential of the TICs was affected by decreasing paracrine factors, such as Wnt2 in the niche cells (Table 1B and Supplementary Table S2). With 10 Wnt responsive TICs, different types of niche cells were associated with different tumor forming frequencies (see Supplementary Table S5 with p-value of 0.03 and Figure 5C). shRNA knockdown resulted in about a 4-fold decrease in tumor forming frequency, as compared to the control shRNA.

Kaplan-Meier curves were also generated for TICs=10 groups in Table 1B (Figure 5D). Across all 8 groups, there is a significant difference between groups ($p<0.001$). In order to test whether shRNA niche cells reduced the time to tumor formation, relative to the control shRNA, four comparisons were undertaken. There was no difference observed between shRNA groups for 0 or 2 niche cells, a marginal difference for 10 niche cells, and a significant difference detected for 20 niche cells (Supplementary Table S6a–d).

In summary, limiting dilution analyses and, alternatively, tumor latency analyses show that niche cells increased both the incidence and decreased the latency of tumor formation in a dose dependent manner, and futhermore, that shRNA knockdown of Wnt2 reduced tumor formation, most noticeably in the presence of increased numbers of niche cells.

Discussion

Intratumoral heterogeneity correlates with clinical outcome (30), which also poses considerable challenges for tumor prognosis and therapy (31). Increasing evidence has emerged to show that various subpopulations of cells within solid tumors may respond differently to both conventional and targeted therapies. In a clinical study, residual breast cancer cells following treatment with either an aromatase inhibitor or chemotherapy showed an enrichment of TIC subpopulation (32). However, whether cells are in a dynamic state under treatment conditions has not been determined. In addition, studies from glioblastoma, in which $CD133^{+}$ has been identified as a stem cell marker, have shown a population of $CD133^{-}$ cells can generate both $CD133^{+}$ and $CD133^{-}$ progeny (33), suggesting a dynamic exchange between the $CD133^{+}$ and $CD133^{-}$ cells. Thus, plasticity has to be considered as a factor that may influence tumor development. However, the mechanisms by which the different types of tumor cells interact with each other during tumor progression remain to be elucidated. Similarly, using the combined analyses of cellular differentiation markers (CD24, CD44, human epidermal growth factor receptor 2 (HER2) etc.) and genotypic alterations such as copy number variation, Polyak and colleagues uncovered a high level of genetic heterogeneity between stem-like cells and more differentiated cancer cell populations. These results questioned the validity of a unidirectional simple differentiation

stem cell hierarchy (34). Therefore, the elucidation of the dynamic and functional relationship between various breast tumor cells may provide new therapeutic targets for drug development with the goal of both preventing breast cancer and reducing relapse, metastasis.

Using both *in vitro* co-culture, transwell-culture and *in vivo* co-transplantation together with the shRNA knockdown technologies, we identified a group of mesenchymal-like tumor cells from the p53 null mammary tumors. Factors that have been reported to function as niche components in various tissues, such as cytokines, chemokines and secretory Wnt proteins, were significantly increased within our mesenchymal-like cell subpopulation. Wnt2 expression has been detected at high levels in both epithelium and stroma in infiltrating carcinomas and fibroadenomas, indicating an autocrine Wnt signaling loop might exist within the tumor cells (35). Stem cells may generate their own niche or interact with the surrounding microenvironment via Wnt signaling (36). We have demonstrated a marked overlap of the Wnt positive cells with the TIC population characterized as $CD29^{H}CD24^{H}$ using a Wnt reporter system (17). Consistently, a decreased self-renewal potential of the TICs when co-transplanted with the niche cells that were transduced with shRNAs mediating knockdown of Wnt2 indicated that the functional interaction between the TICs and the niche cells was disrupted. Thus, these various cell types functionally interact with each other using a mechanism similar to that employed in the normal mammary gland. CXCL12 together with its receptor CXCR4 constitutes the chemokine/receptor axis that plays an important role in mammary tumorigenicity and metastasis (37). The interaction between CXCL12 and CXCR4 also plays an important role in maintaining the hematopoietic stem cell pool in the bone marrow (38). CXCL12 is also expressed in the cytoplasm of the malignant ovarian epithelial cells (39). In our study, the ligand CXCL12 and its receptor, CXCR4, are highly expressed, respectively, in the tumor-derived niche cells and the TICs, suggesting the possible interaction between TICs and the mesenchymal like niche. Therefore, the knockdown of both CXCR4 in the TICs and the CXCL12 in the niche subpopulation were performed in order to investigate the role of CXCL12 and CXCR4 in the interaction of our various tumor cells. The reduction in the mammosphere forming efficiency when Wnt2/Fzd7 were knocked down is not as dramatic as that in the Cxcl12/Cxcr4 knockdown (Figures 4G&4H) although the expression level of Fzd7 was decreased by 70% as compared to 50% for Cxcr4 (Figures 4E&4F). This most likely is due to the presence of multiple redundant ligand/receptor components for Wnt signaling as compared to the specific interaction between CXCL12 and CXCR4.

Our data also support a role for IL6 in TIC self-renewal as demonstrated by the reduced mammosphere forming ability observed following IL6 knockdown. These results are consistent with previous findings that IL6 regulates the breast TIC population through both autocrine and paracrine mechanisms (40, 41). Tumor cells have been shown to secrete IL-6 to promote tumor growth (42) via an autocrine mechanism. It is also likely that the TICs produce factors that regulate the mesenchymal population. However, the level of CXCL12 secretion was extremely low when TICs were cultured alone suggested that a potential paracrine feedback pathway regulating CXCL12 expression may be important in this tumor model.

Both tumor formation frequency and tumor latency time after limiting dilution transplantation experiments reflect the process of tumor initiation, with the formation frequency representing the relative number of stem cells and/or the ability of the cell population to establish a niche to allow replication, while tumor latency represents the proliferative potential of these cells. In vivo co-transplantation demonstrated that such niche cells enhanced TICs tumor initiation likely by providing an improved microenvironment, especially for those tumors initiated from extremely low numbers of the TICs. The shortened latency observed in the presence of niche cells is consistent with the findings that Wnt signaling promotes cell proliferation (43).

While studies have suggested that there is a dynamic equilibrium among various cell subpopulations it is unknown the relevance of this “plasticity” in influencing treatment response, metastasis, and recurrence (44). It remains to be determined what factors contribute to intratumoral heterogeneity in solid cancers, and if plasticity in these subpopulations contributes to treatment resistance, metastasis, minimal residual disease and recurrence. One method to define self-renewal and differentiation properties of cancer stem cells is through limiting dilution transplantation to identify cells capable of forming tumors that recapitulate the characteristics of the original tumor. Our results suggest that p53 null tumors contain cells with different degrees of self-renewal capacity. While cell plasticity may exist between TICs and non-TICs, a majority of the resulting tumor cells were derived from the TICs (Supplementary Figure S6 and Figure 6 (1)). Mesenchymal cells resulting from an EMT are usually more migratory and less proliferative than their epithelial counterparts (45). Thus, it is likely that the widely used limiting dilution transplantation assay may preferentially identify the rapidly proliferative TICs, but not the less proliferative, more quiescent population that may also initiate tumor growth. Previous limiting dilution transplantation assays have shown that the niche cell population is 30-fold less tumorigenic than the TICs (17), and the niche cells, indeed, are more quiescent and less proliferative than the TICs. Notwithstanding these studies, in the absence of appropriate lineage tracing experiments, it is not feasible to definitively know the origin of these primary tumor cells. When TICs were co-transplanted with the mesenchymal-like tumor cells, the mesenchymal-like tumor cells increased the self-renewal and tumorigenic potential of the TICs, causing the expansion of the TIC population especially during the early tumor development (Figure 6 (2)). $CD29^{H}CD24^{L}$ cells fail to generate tumors with a low number of cells, and the resulting tumors exhibit a different phenotype and FACS profile as compared to the TIC-derived tumors, suggesting that these cancer cell subpopulations may interact and collaborate differently with the host microenvironment. Interactions of self-renewing tumor cells both with the microenvironment and surrounding tumor cells determine the progression and phenotypic features of the tumors. The generation of the cells with less self-renewal, but with mesenchymal feature was able to fuel tumor growth. Recently, using approaches including whole genome sequencing, and reverse phase protein arrays (RPPA), Li et al (46) thoroughly characterized 13 patient-derived xenograft (PDX) lines along with their advanced primary breast tumors. The studies showed that while PDXs have relatively stable genomes without a significant accumulation of DNA structural rearrangements, minor mutant clones are retained in PDXs during multiple transplants, indicating the possibility of cooperation of clones during tumor evolution. Further characterization of the individual

subpopulations using PDX lines will help us better understand the complexity of the human breast cancer. Eliminating multiple subpopulations, and blocking the transition between these populations will be an important consideration when designing effective cancer therapies.

Only a limited number of studies to date have been able to demonstrate the importance of functional intratumoral heterogeneity. For example, Gunther and colleagues reported recently that both the luminal and basal populations were required for efficient tumor formation in the MMTV-driven Wnt1 genetically engineered mouse model, which was dependent on luminal Wnt1 expression (47). In this transgenic mouse model Hras mutations were used as clonal markers identifying both distinct basal Hras mutant and luminal wild type tumor subclones. A similar requirement for Wnt signaling was observed in our stochastic p53 null Balb/c tumors that are also a model for basal-like breast cancer (25). However, in the p53 model a distinct TIC population has been identified, and as discussed previously the interaction with the mesenchymal-like subpopulation enhanced, but was not essential for tumor formation.

To better understand clonal heterogeneity, Polyak and colleagues recently developed an experimental model in which factors previously implicated in tumor progression were overexpressed in the indolent MDA-MB-468 cell line. These investigators then generated sub-lines expressing different cytokines and used these to model how sub-clonal cooperation was required for metastasis (48). These studies support the conclusion that there are non-cell autonomous drivers of tumor growth, and importantly that inter-clonal interactions can lead to new phenotypic properties.

In our studies, no large-scale genomic deletions or insertions among individual subpopulations of $CD29^{H}CD24^{H}$, $CD29^{H}CD24^{L}$, $CD29^{L}CD24^{H}$ and $CD29^{L}CD24^{L}$ were detected using CGH analysis. Therefore, in the p53 null Balb/c tumors it appears that epigenetic factors may influence clonal heterogeneity, and that intratumoral heterogeneity may not be exclusively due to genetic differences among various subpopulations. Thus, epigenetic modifications may allow them to develop into cells with both markedly different tumorigenic potential, as well as to become different types of cells when they give rise to phenotypically different tumors when introduced into the similar microenvironment. DNA sequencing has demonstrated an increased mutation frequency in human triple negative breast cancers as compared to ER positive luminal breast cancers (49), but many of these mutations occurred at low frequency. So it is likely that both genetic and epigenetic factors will play a role in generating intratumoral heterogeneity and this may only be detected by in depth single cell sequencing. It is also likely that the stochastic tumors resulting in the germline p53 null mouse model are under different selection pressures from those observed in somatic p53 null and mutant human breast cancers.

Materials and Methods

Materials

TOP-eGFP, and its control vector, FOP-eGFP, were kind gifts from Dr. Irving. Weissman (Stanford University, Stanford, CA). pEIZsGreen and pEITomato Red vectors were kindly

provided by Dr. Bryan Welm (Oklahoma Medical Research Foundation, Oklahoma City, OK). The highly transfectable 293T cell line, which was used routinely for virus propagation, was purchased from ATCC. No test and authentication was done by the authors. All other antibodies, lentiviral particles, and primers were purchased from commercial sources as listed in SI "Materials and Methods".

Preparation of single mammary tumor cells

Mice were maintained in accordance with the National Institutes of Health Guide for the Care and Use of Experimental Animals. All animal protocols were reviewed and approved by the Animal Protocol Review Committees of University of Pittsburgh and Baylor College of Medicine. P53 null mammary tumors were generated as previously described (20).

Mammosphere and transwell co-culturing assays

The protocol for mammosphere assays was as described by Dontu (14) and in SI.

For mammosphere co-culture, 5,000 TICs, 5,000 $CD29^{H}CD24^{L}$ niche cells, or 2,500 TICs plus 2,500 niche cells, 2,500 TICs plus 2,500 $CD29^{L}$ cells, or 2,500 TICs plus 2,500 niche cells with Cxcl12 or Wnt2 knockdown, and 2,500 TICs with Cxcr4 or Fzd7 knockdown plus 2,500 niche cells were cultured after dissociation of the primary mammospheres in 2 ml serum-free mammosphere medium under a non-adherent condition for 7 days. PKH26 (Red fluorescence) and PKH67 (Green fluorescence) cell linker kits (Sigma) were used to label individual cell subpopulations according to manufacturer's protocol.

For transwell culture of mammospheres, 5,000 TICs, 5,000 $CD29^{H}CD24^{L}$ niche cells, or 2,500 TICs plus 2,500 niche cells were transwell cultured with 5,000 dissociated TICs after dissociation of the designated cell types from the primary mammospheres in 3.6 ml serum-free mammosphere medium under a non-adherent condition in Transwell plates (Corning, NY) for 7 days.

Lentiviral transduction

Lentiviral transduction was performed as described (17). The pEIZsGreen and pEITomato Red lentivirus reporters were driven by an EF1α promoter, and the lentiviruses were packaged in 293T cells by co-transfection of pEIZsGreen (or pEITomato Red), pRSV-rev, pMDLg-pRRE and pCMV-VSVG using Fugene transfection reagent (Roche, Indianapolis, IN). For bioluminescence tracking, enzymatically digested p53 null tumor cells (20,000/per well) were suspended into 24-well ultra low attachment plates, and transduced with lentiviruses expressing either pEIZsGreen or pEITomato Red allowing stable integration of ZsGreen and Tomato Red fluorescence reporter at a multiplicity of infection (MOI) of 10, respectively, for 24 hrs in a final volume of 1 ml serum-free mammosphere medium. After transduction, ZsGreen or Tomato Red positive cells were FACS sorted and collected in HBSS medium, prior to transplantation.

For knockdown analysis, dissociated and FACS sorted TICs and niche cells from the p53 null tumors (20,000/per well) were suspended into 24-well ultra low attachment plates, and were transfected with empty shRNA vector control, panels of shRNA lentiviruses against

Cxcr4, Fzd7, or two different Wnt2 shRNA lentiviruses, one Cxcl12 shRNA, and two different Il6 shRNA lenviruses, respectively as designated in the main text, for 48–72 hrs in a final volume of 1 ml serum-free mammosphere medium. The shRNA sequences (antisense) used in this study are listed in SI. Cells infected with viruses were selected in the presence of 2 ug/ml puromycin. Downregulation of the target genes were verified by RT-PCR using Taqman primer and probe sets (Life Technologies, Grand Island, NY). Lentiviral pLKO.1 empty vector control (Dharmacon, Lafayette, CO) was used as the control vector.

In vivo transplantation into the cleared mammary fat pad

Clearance of mammary fat pad and transplantation procedures were performed as originally described (20). For co-transplantation studies, FACS sorted $CD29^{H}CD24^{L}$ cells and TICs were mixed at designated numbers in HBSS medium.

FACS-sorted TICs and niche cells were also collected and transfected with lentiviruses as described in **Lentiviral transduction**. Then these two populations of cells were mixed and co-transplanted into the cleared fat pads of 3-wk-old female recipient mice (Balb/C mice from Harlan) at the designated ratios of 200/0, 120/80, 68/132, and 32/168 (with a total number of cells of 200). The resulting tumors were FACS analyzed based on expression of ZsGreen and TomatoRed.

For gene knockdown studies, after transduction with the anti-Wnt2, the designated number of cells were washed once with 1 X PBS and co-transplanted with the freshly sorted Wnt responsive GFP positive cells into the cleared fat pads of 3-wk-old female Balb/C mice. For all in vivo transplantation assays, 50% Growth Factor Reduced Matrigel (BD Biosciences, San Jose, CA) was added to make the final volume of 2 μl prior to injection. Two weeks after transplantation, tumor formation was monitored daily. Mammary tumor tissues were removed when tumor size reached 1cm in diameter.

Quantitative reverse transcriptase –polymerase chain reaction (qRT-PCR)

RNA (300 ng) each was used to generate cDNA with the High Capacity cDNA Reverse Transcription Kit (Applied Biosystems) according to the company's protocol. qRT-PCR reactions were performed as described in SI.

Immunostaining and microscopic analysis

Paraffin embedded and paraformaldehyde (PFA) fixed tumor tissues, and FACS sorted and cytospun cells were stained with the antibodies against K5 (1:5,000), SMA (1:250) and Ki67 (1:200) as described in SI. Microscopic analysis was done on an Olympus BMAX 50 fluorescence microscope with details described in SI.

Microarray analysis

Statistical analyses for microarray were performed in the biostatistics core facility of the Dan L. Duncan Cancer Center at Baylor College of Medicine (A.T.), and University of North Caroline (C.F.). Detailed analysis was described in (20) and in SI. The complete array data can be accessed at Gene Expression Omnibus (GEO, GSE8863).

Mesenchymal and claudin-low signature analysis on individual populations

RNA microarray data obtained from the four individual subpopulations ($CD29^{H}CD24^{H}$, $CD29^{H}CD24^{L}$, $CD29^{L}CD24^{H}$, $CD29^{L}CD24^{L}$) were analyzed. Each signature/module was built using the median expression of the gene lists published in corresponding papers as referenced. Boxplots of the signatures were constructed and ANOVA analysis for the signatures in the 4 different groups was performed using the R software package. Three independent tumors from the p53 null model were included in this analysis, for each box plot category.

Supplementary Material

Refer to Web version on PubMed Central for supplementary material.

Acknowledgments

We would like to thank Dr. Irving Weissman for proving the TOP-eGFP, FOP-eGFP Wnt reporter vectors, Dr. Bryan Welm for providing the pEIZsGreen and pEITomato Red constructs, and Dr. Wei-Wen Cai for the BAC-based CGH array analysis. We would like to thank the Cytometry Facility at the University of Pittsburgh Cancer Institute, the Flow Cytometry Core at Magee-Womens Research Institute, and Cytometry and Cell Sorting Core at Baylor College of Medicine (BCM). The graphic illustration for Figure 6 is provided by Alec Sarkas, University of Pittsburgh. We would also like to thank Dr. Adrian Lee (University of Pittsburgh) for constructive criticisms on this manuscript.

Grant Support

This work was supported by grants including NIH/NCI Pathway to Independence (PI) Award CA14289 (MZ); BCM Cancer Center CA125123 (SGH), NCI grants CA148761(JMR), CA149196 (JMR), NCI Breast SPORE program P50-CA58223-09 (CMP), and by the Breast Cancer Research Foundation (CMP). This project used the UPCI Cytometry Facility that is supported in part by award P30CA047904. This work was also conducted with the help of the BCM Cytometry and Cell Sorting Core (NIH P30 AI036211, P30 CA125123, and S10 RR024574), the Genomics and RNA Profiling Core (DK56338), and the Dan L. Duncan Cancer Center grant CA125123 (Osborne).

References

1. Rosen JM, Roarty K. Paracrine signaling in mammary gland development: what can we learn about intratumoral heterogeneity? Breast Cancer Res. 2014; 16:202. [PubMed: 24476463]
2. Forster N, Saladi SV, van Bragt M, Sfondouris ME, Jones FE, Li Z, et al. Basal Cell Signaling by p63 Controls Luminal Progenitor Function and Lactation via NRG1. Dev Cell. 2014; 28:147–60. [PubMed: 24412575]
3. Katona TM, Jones TD, Wang M, Eble JN, Billings SD, Cheng L. Genetically heterogeneous and clonally unrelated metastases may arise in patients with cutaneous melanoma. Am J Surg Pathol. 2007; 31:1029–37. [PubMed: 17592269]
4. Maley CC, Galipeau PC, Finley JC, Wongsurawat VJ, Li X, Sanchez CA, et al. Genetic clonal diversity predicts progression to esophageal adenocarcinoma. Nat Genet. 2006; 38:468–73. [PubMed: 16565718]
5. Nowell PC. The clonal evolution of tumor cell populations. Science. 1976; 194:23–8. [PubMed: 959840]
6. Nik-Zainal S, Van Loo P, Wedge DC, Alexandrov LB, Greenman CD, Lau KW, et al. The life history of 21 breast cancers. Cell. 2012; 149:994–1007. [PubMed: 22608083]
7. Clarke MF, Dick JE, Dirks PB, Eaves CJ, Jamieson CH, Jones DL, et al. Cancer stem cells–perspectives on current status and future directions: AACR Workshop on cancer stem cells. Cancer research. 2006; 66:9339–44. [PubMed: 16990346]
8. Almendro V, Marusyk A, Polyak K. Cellular heterogeneity and molecular evolution in cancer. Annual review of pathology. 2013; 8:277–302.

9. Kreso A, O'Brien CA, van Galen P, Gan OI, Notta F, Brown AM, et al. Variable clonal repopulation dynamics influence chemotherapy response in colorectal cancer. Science. 2013; 339:543–8. [PubMed: 23239622]
10. Campbell PJ, Pleasance ED, Stephens PJ, Dicks E, Rance R, Goodhead I, et al. Subclonal phylogenetic structures in cancer revealed by ultra-deep sequencing. Proceedings of the National Academy of Sciences of the United States of America. 2008; 105:13081–6. [PubMed: 18723673]
11. Navin N, Kendall J, Troge J, Andrews P, Rodgers L, McIndoo J, et al. Tumour evolution inferred by single-cell sequencing. Nature. 2011; 472:90–4. [PubMed: 21399628]
12. Gerlinger M, Rowan AJ, Horswell S, Larkin J, Endesfelder D, Gronroos E, et al. Intratumor heterogeneity and branched evolution revealed by multiregion sequencing. The New England journal of medicine. 2012; 366:883–92. [PubMed: 22397650]
13. Lobo NA, Shimono Y, Qian D, Clarke MF. The biology of cancer stem cells. Annu Rev Cell Dev Biol. 2007; 23:675–99. [PubMed: 17645413]
14. Dontu G, Abdallah WM, Foley JM, Jackson KW, Clarke MF, Kawamura MJ, et al. In vitro propagation and transcriptional profiling of human mammary stem/progenitor cells. Genes Dev. 2003; 17:1253–70. [PubMed: 12756227]
15. Li X, Lewis MT, Huang J, Gutierrez C, Osborne CK, Wu MF, et al. Intrinsic resistance of tumorigenic breast cancer cells to chemotherapy. J Natl Cancer Inst. 2008; 100:672–9. [PubMed: 18445819]
16. Atkinson RL, Zhang M, Diagaradjane P, Peddibhotla S, Contreras A, Hilsenbeck SG, et al. Thermal enhancement with optically activated gold nanoshells sensitizes breast cancer stem cells to radiation therapy. Sci Transl Med. 2010; 2:55ra79.
17. Zhang M, Atkinson RL, Rosen JM. Selective targeting of radiation-resistant tumor-initiating cells. Proc Natl Acad Sci U S A. 2010; 107:3522–7. [PubMed: 20133717]
18. Yang G, Quan Y, Wang W, Fu Q, Wu J, Mei T, et al. Dynamic equilibrium between cancer stem cells and non-stem cancer cells in human SW620 and MCF-7 cancer cell populations. Br J Cancer. 2012; 106:1512–9. [PubMed: 22472879]
19. Li L, Clevers H. Coexistence of quiescent and active adult stem cells in mammals. Science. 2010; 327:542–5. [PubMed: 20110496]
20. Zhang M, Behbod F, Atkinson RL, Landis MD, Kittrell F, Edwards D, et al. Identification of tumor-initiating cells in a p53-null mouse model of breast cancer. Cancer Res. 2008; 68:4674–82. [PubMed: 18559513]
21. Morrison SJ, Spradling AC. Stem cells and niches: mechanisms that promote stem cell maintenance throughout life. Cell. 2008; 132:598–611. [PubMed: 18295578]
22. Li J, Jiang T, Mao JH, Balmain A, Peterson L, Harris C, et al. Genomic segmental polymorphisms in inbred mouse strains. Nat Genet. 2004; 36:952–4. [PubMed: 15322544]
23. Cai WW, Mao JH, Chow CW, Damani S, Balmain A, Bradley A. Genome-wide detection of chromosomal imbalances in tumors using BAC microarrays. Nat Biotechnol. 2002; 20:393–6. [PubMed: 11923847]
24. Fan C, Prat A, Parker JS, Liu Y, Carey LA, Troester MA, et al. Building prognostic models for breast cancer patients using clinical variables and hundreds of gene expression signatures. BMC Med Genomics. 2011; 4:3. [PubMed: 21214954]
25. Pfefferle AD, Herschkowitz JI, Usary J, Harrell JC, Spike BT, Adams JR, et al. Transcriptomic classification of genetically engineered mouse models of breast cancer identifies human subtype counterparts. Genome Biol. 2013; 14:R125. [PubMed: 24220145]
26. Herschkowitz JI, Simin K, Weigman VJ, Mikaelian I, Usary J, Hu Z, et al. Identification of conserved gene expression features between murine mammary carcinoma models and human breast tumors. Genome Biol. 2007; 8:R76. [PubMed: 17493263]
27. Zeng YA, Nusse R. Wnt proteins are self-renewal factors for mammary stem cells and promote their long-term expansion in culture. Cell Stem Cell. 2010; 6:568–77. [PubMed: 20569694]
28. Liu S, Ginestier C, Ou SJ, Clouthier SG, Patel SH, Monville F, et al. Breast cancer stem cells are regulated by mesenchymal stem cells through cytokine networks. Cancer Res. 2011; 71:614–24. [PubMed: 21224357]

29. Gatti M, Pattarozzi A, Bajetto A, Wurth R, Daga A, Fiaschi P, et al. Inhibition of CXCL12/CXCR4 autocrine/paracrine loop reduces viability of human glioblastoma stem-like cells affecting self-renewal activity. Toxicology. 2013; 314:209–20. [PubMed: 24157575]
30. Almendro V, Cheng YK, Randles A, Itzkovitz S, Marusyk A, Ametller E, et al. Inference of Tumor Evolution during Chemotherapy by Computational Modeling and In Situ Analysis of Genetic and Phenotypic Cellular Diversity. Cell Rep. 2014
31. Patel AP, Tirosh I, Trombetta JJ, Shalek AK, Gillespie SM, Wakimoto H, et al. Single-cell RNA-seq highlights intratumoral heterogeneity in primary glioblastoma. Science. 2014; 344:1396–401. [PubMed: 24925914]
32. Creighton CJ, Li X, Landis M, Dixon JM, Neumeister VM, Sjolund A, et al. Residual breast cancers after conventional therapy display mesenchymal as well as tumor-initiating features. Proc Natl Acad Sci U S A. 2009; 106:13820–5. [PubMed: 19666588]
33. Chen R, Nishimura MC, Bumbaca SM, Kharbanda S, Forrest WF, Kasman IM, et al. A hierarchy of self-renewing tumor-initiating cell types in glioblastoma. Cancer Cell. 2010; 17:362–75. [PubMed: 20385361]
34. Park SY, Gonen M, Kim HJ, Michor F, Polyak K. Cellular and genetic diversity in the progression of in situ human breast carcinomas to an invasive phenotype. J Clin Invest. 2010; 120:636–44. [PubMed: 20101094]
35. Dale TC, Weber-Hall SJ, Smith K, Huguet EL, Jayatilake H, Gusterson BA, et al. Compartment switching of WNT-2 expression in human breast tumors. Cancer Res. 1996; 56:4320–3. [PubMed: 8813115]
36. Clevers H, Loh KM, Nusse R. Stem cell signaling. An integral program for tissue renewal and regeneration: Wnt signaling and stem cell control. Science. 2014; 346:1248012. [PubMed: 25278615]
37. Li YM, Pan Y, Wei Y, Cheng X, Zhou BP, Tan M, et al. Upregulation of CXCR4 is essential for HER2-mediated tumor metastasis. Cancer Cell. 2004; 6:459–69. [PubMed: 15542430]
38. Levesque JP, Hendy J, Takamatsu Y, Simmons PJ, Bendall LJ. Disruption of the CXCR4/CXCL12 chemotactic interaction during hematopoietic stem cell mobilization induced by GCSF or cyclophosphamide. J Clin Invest. 2003; 111:187–96. [PubMed: 12531874]
39. Machelon V, Gaudin F, Camilleri-Broet S, Nasreddine S, Bouchet-Delbos L, Pujade-Lauraine E, et al. CXCL12 expression by healthy and malignant ovarian epithelial cells. BMC Cancer. 2011; 11:97. [PubMed: 21410972]
40. Sansone P, Storci G, Tavolari S, Guarnieri T, Giovannini C, Taffurelli M, et al. IL-6 triggers malignant features in mammospheres from human ductal breast carcinoma and normal mammary gland. J Clin Invest. 2007; 117:3988–4002. [PubMed: 18060036]
41. Korkaya H, Kim GI, Davis A, Malik F, Henry NL, Ithimakin S, et al. Activation of an IL6 inflammatory loop mediates trastuzumab resistance in HER2+ breast cancer by expanding the cancer stem cell population. Mol Cell. 2012; 47:570–84. [PubMed: 22819326]
42. Gao SP, Mark KG, Leslie K, Pao W, Motoi N, Gerald WL, et al. Mutations in the EGFR kinase domain mediate STAT3 activation via IL-6 production in human lung adenocarcinomas. J Clin Invest. 2007; 117:3846–56. [PubMed: 18060032]
43. van de Wetering M, Sancho E, Verweij C, de Lau W, Oving I, Hurlstone A, et al. The beta-catenin/TCF-4 complex imposes a crypt progenitor phenotype on colorectal cancer cells. Cell. 2002; 111:241–50. [PubMed: 12408868]
44. Akunuru S, James Zhai Q, Zheng Y. Non-small cell lung cancer stem/progenitor cells are enriched in multiple distinct phenotypic subpopulations and exhibit plasticity. Cell Death Dis. 2012; 3:e352. [PubMed: 22825470]
45. Rubio CA. Further studies on the arrest of cell proliferation in tumor cells at the invading front of colonic adenocarcinoma. Journal of gastroenterology and hepatology. 2007; 22:1877–81. [PubMed: 17914963]
46. Li S, Shen D, Shao J, Crowder R, Liu W, Prat A, et al. Endocrine-therapy-resistant ESR1 variants revealed by genomic characterization of breast-cancer-derived xenografts. Cell Rep. 2013; 4:1116–30. [PubMed: 24055055]

47. Cleary AS, Leonard TL, Gestl SA, Gunther EJ. Tumour cell heterogeneity maintained by cooperating subclones in Wnt-driven mammary cancers. Nature. 2014; 508:113–7. [PubMed: 24695311]

48. Marusyk A, Tabassum DP, Altrock PM, Almendro V, Michor F, Polyak K. Non-cell-autonomous driving of tumour growth supports sub-clonal heterogeneity. Nature. 2014

49. Wang Y, Waters J, Leung ML, Unruh A, Roh W, Shi X, et al. Clonal evolution in breast cancer revealed by single nucleus genome sequencing. Nature. 2014; 512:155–60. [PubMed: 25079324]

Statement of significance

Intratumoral heterogeneity has been considered one important factor in assessing a patient's initial response to treatment and selecting drug regimens to effectively increase tumor response rate. Elucidating the functional interactions between various subpopulations of tumor cells will help provide important new insights in understanding treatment response and tumor progression.

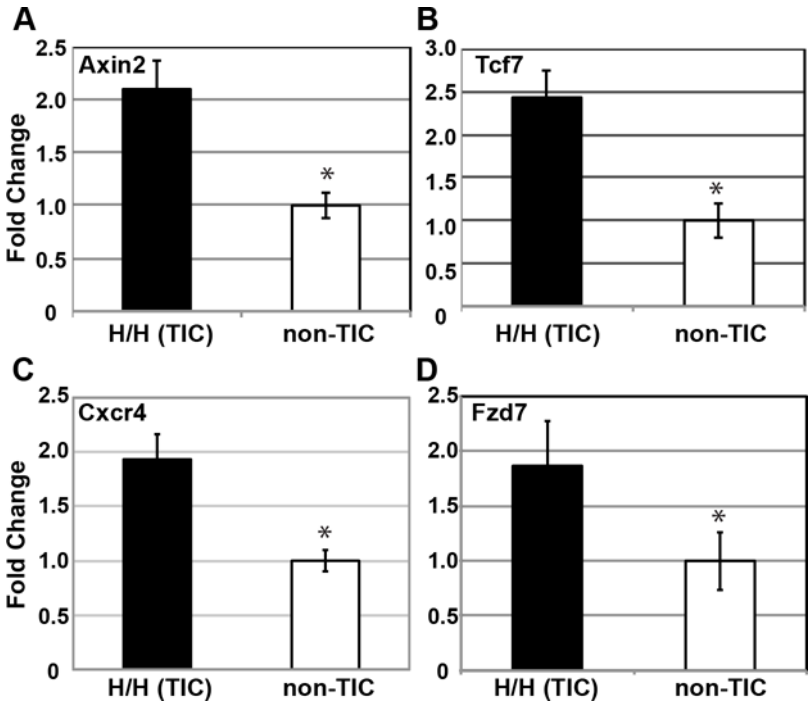

Figure 1. qPCR analysis using p53 null tumors suggested (A) Axin2, (B) Tcf7, (C) Fzd7 and (D) Cxcr4 were upregulated in TICs

Total RNA isolated from FACS-sorted subpopulations based upon the expression of CD29 and CD24 were extracted using the RNA purification kit as mentioned in SI "Microarray Analysis". *p<0.01.

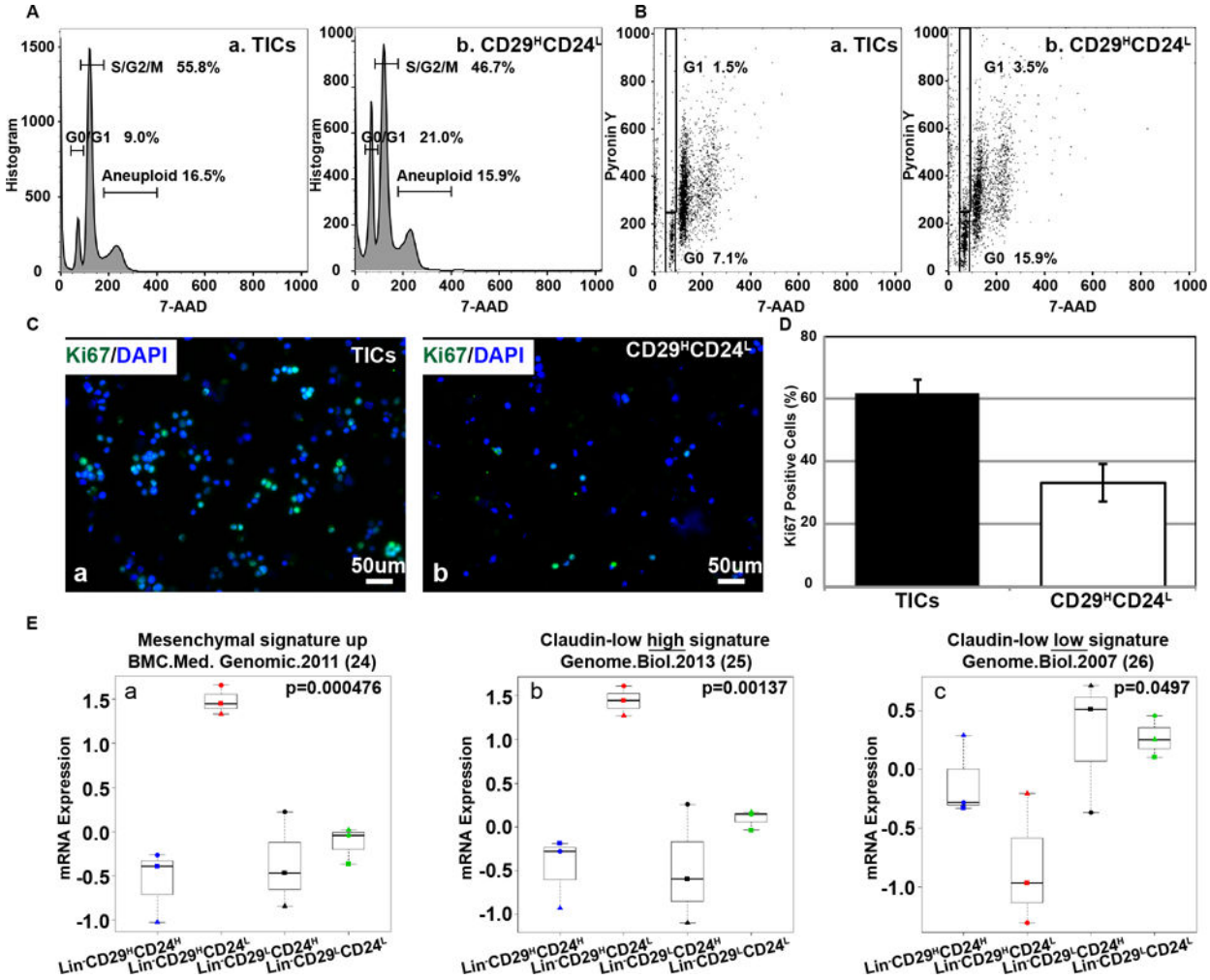

Figure 2. Molecular characterization of the individual tumor cell subpopulations

(A) and (B) Cell cycle analyses of the FACS sorted TIC (2Aa, 2Ba) and $CD29^{H}CD24^{L}$ (2Ab, 2Bb) subpopulations. (C) The cells (a. TICs; b. $CD29^{H}CD24^{L}$) were also cytospun and analyzed using an antibody against Ki67. (D) Quantification of Ki67-positive cells within the TIC and niche populations**. (**E) The $CD29^{H}CD24^{L}$ niche population has features of mesenchymal cells and claudin-low tumors. The $CD29^{H}CD24^{L}$ population expresses (Ea) core mesenchymal signature, (Eb) claudin-low high gene expression signature, and (Ec) claudin-low low gene expression signature as compared with all three other populations. Individual subpopulations of RNAs were isolated from pooled tumors of the same subtypes after FACS isolation. Three independent p53 null tumors (T1 ▪; T2 ● T7 ▲) were included. $CD29^{H}CD24^{H}$ (Blue), $CD29^{H}CD24^{L}$ (Red), $CD29^{L}CD24^{H}$ (Black) and $CD29^{L}CD24^{L}$ (green).

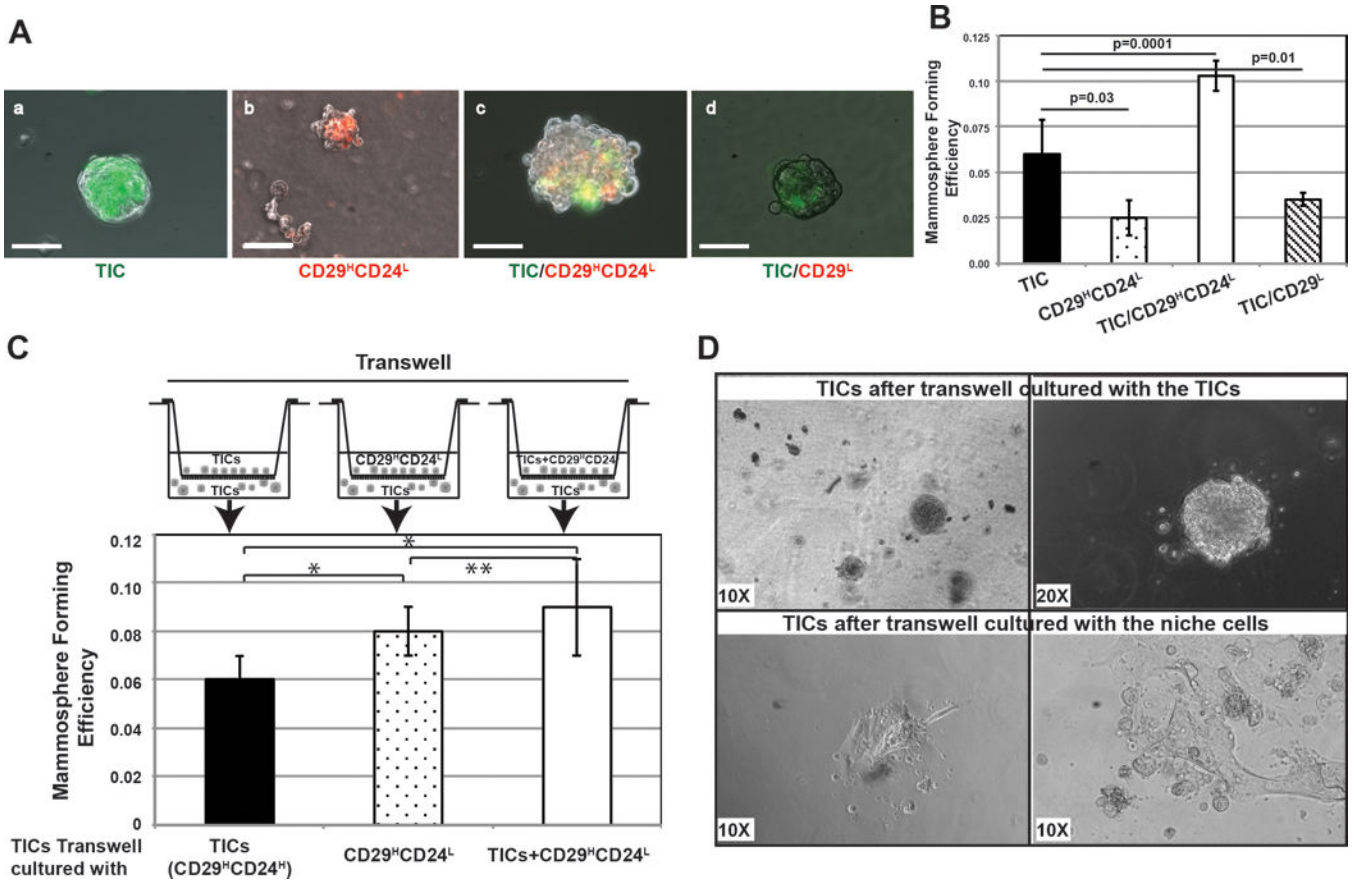

Figure 3. Co-culture and transwell-culture of TICs with CD29^{H}CD24^{L} cells or CD29^{L} cells

All cells used were dissociated from the primary mammosphere culture and labeled with green: PKH67 fluorescence or red: PKH26 fluorescence as designated. (A) and (B) Co-culture of TICs and CD29^{H}CD24^{L} cells display larger and an increased number of mammospheres compared with their individual cultures alone. (Aa) TICs (Green); (Ab) CD29^{H}CD24^{L} (Red); (Ac) TICs (Green) and CD29^{H}CD24^{L} (Red) were mixed; (Ad) TICs (Green) and CD29^{L}(Red) were mixed. (B) Mammosphere forming efficiency of TICs cultured alone, CD29^{H}CD24^{L} alone, a mixture of TICs and CD29^{H}CD24^{L}, and a mixture of TICs and CD29^{L}. Six repeats for each group. T1 tumors were used in the study. Mammosphere formation was determined and quantitated at day 7. (C) and (D) Transwell-cultures of the CD29^{H}CD24^{L} and TICs display increased self-renewal and differentiation potential of the TICs. (C) TICs, CD29^{H}CD24^{L} niche cells, and a mixture of TICs and niche cells were transwell cultured with dissociated TICs from the primary mammospheres in serum-free mammosphere medium under a non-adherent condition for 7 days. Mammosphere formation was determined and quantitated as above at day 7. *<0.05, ** p>0.05. (D) Mammospheres formed from the TICs after transwell culturing with the TICs or niche cells were collected, and transferred to the 8-well chamber slides precoated with the Growth Factor Reduced Matrigel. Pictures were taken after 14 days. Scale bar, 50 μm.

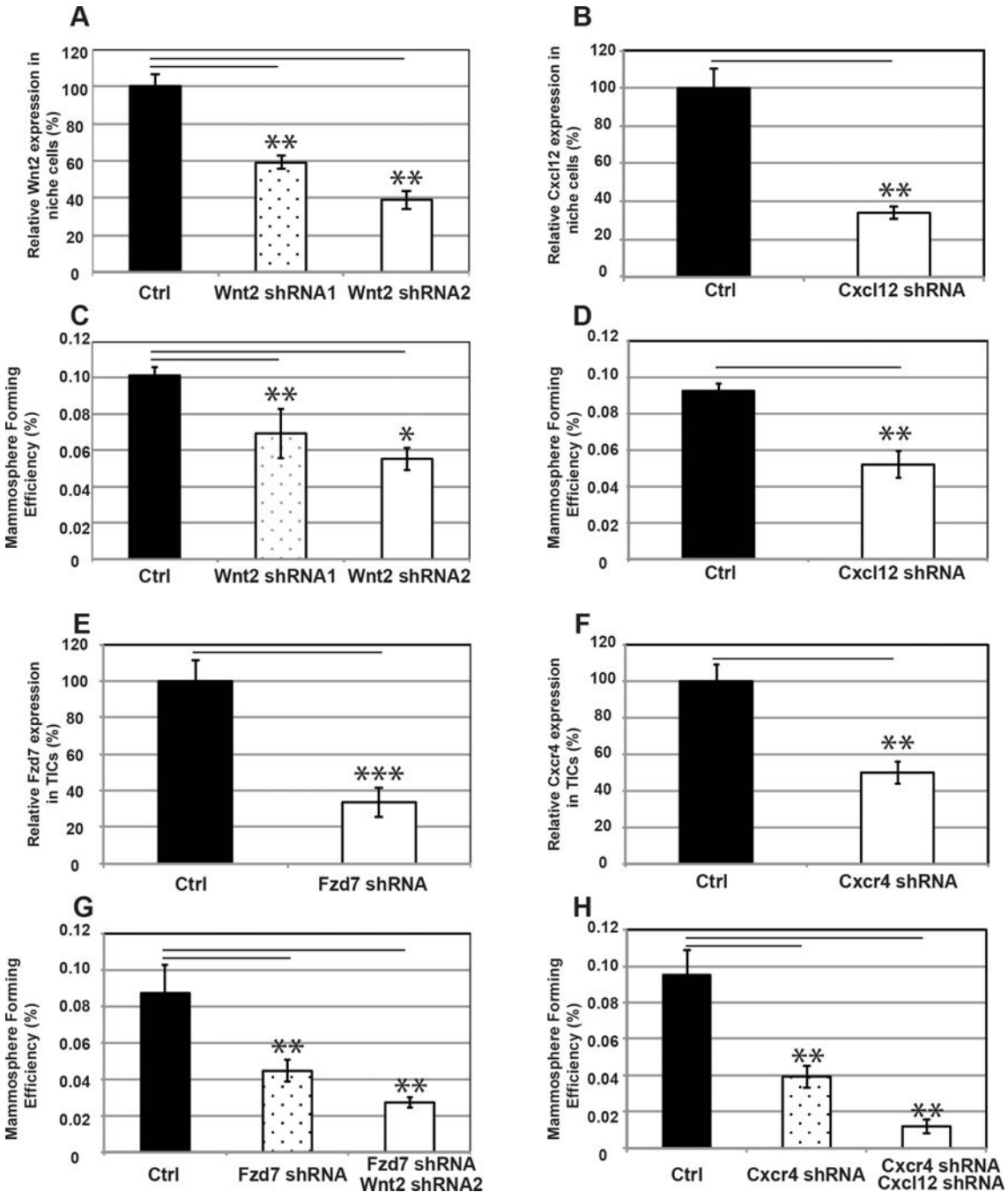

Figure 4. Inhibition of Wnt2 and Cxcl12 signaling in the niche cells, and Fzd7 and Cxcr4 in the TICs with shRNAs, respectively, reduced the self-renewal of the TICs

(A) and (B) Wnt2 and Cxcl12 shRNA lentiviruses (shRNA) and control lentivirus (Ctrl) were introduced into the dissociated $CD29^{H}CD24^{L}$ after being FACS sorted from p53 null T1 tumors. After 72 hrs of selection with puromycin, levels of Wnt2 and Cxcl12 were determined by qPCR. (C) and (D) Dissociated tumor niche cells from T1 tumor, infected with control and Wnt2-shRNA or Cxcl12-shRNA were plated under mammosphere condition. The designated dissociated single cells from the primary sphere culture were co-cultured with the dissociated TICs cells after primary culture in the mammosphere medium.

▪ TICs were co-cultured with control ($CD29^{H}CD24^{L}$ infected with the empty vector); TICs were co-cultured with $CD29^{H}CD24^{L}$ infected with Wnt2 shRNA1 (C); TICs were co-cultured with $CD29^{H}CD24^{L}$ infected with Wnt2 shRNA2 (C) or Cxcl12 shRNA (D). (E) and (F) Fzd7 and Wnt2 shRNA lentiviruses (shRNA) and control lentivirus (Ctrl) were introduced into the dissociated TICs after being FACS sorted from p53 null T1 tumors. After 72 hrs of selection with puromycin, levels of Fzd7 and Cxcr4 were determined by qPCR. (G) Dissociated tumor cells from T1 tumor, infected with control and Fzd7-shRNA, were plated under mammosphere condition. The dissociated cells were then co-cultured with niche cells either infected with the empty vectors or with Wnt2-shRNA, respectively after primary mammosphere culture, in the mammosphere medium. ▪ TICs infected with the control vector were co-cultured with $CD29^{H}CD24^{L}$ infected with the empty control vector; TICs infected with Fzd7 shRNA were co-cultured with $CD29^{H}CD24^{L}$ infected with the control shRNA; TICs infected with Fzd7 shRNA were co-cultured with $CD29^{H}CD24^{L}$ infected with Wnt2 shRNA. (H) Dissociated tumor cells from T1 tumor, infected with control and Cxcr4-shRNA were plated under mammosphere condition. The dissociated cells were then co-cultured with niche cells either infected with the empty vectors or with Cxcl12-shRNA, respectively after primary mammosphere culture, in the mammosphere medium. ▪ TICs infected with the control vector were co-cultured with $CD29^{H}CD24^{L}$ infected with the empty control vector; TICs infected with Cxcr4 shRNA were co-cultured with $CD29^{H}CD24^{L}$ infected with the control shRNA; TICs infected with Cxcr4 shRNA were co-cultured with $CD29^{H}CD24^{L}$ infected with Cxcl12 shRNA. Three repeats for each group (N=3). The number of mammospheres formed was determined and quantitated at day 7. *<0.0002. **<0.01. ***<0.02.

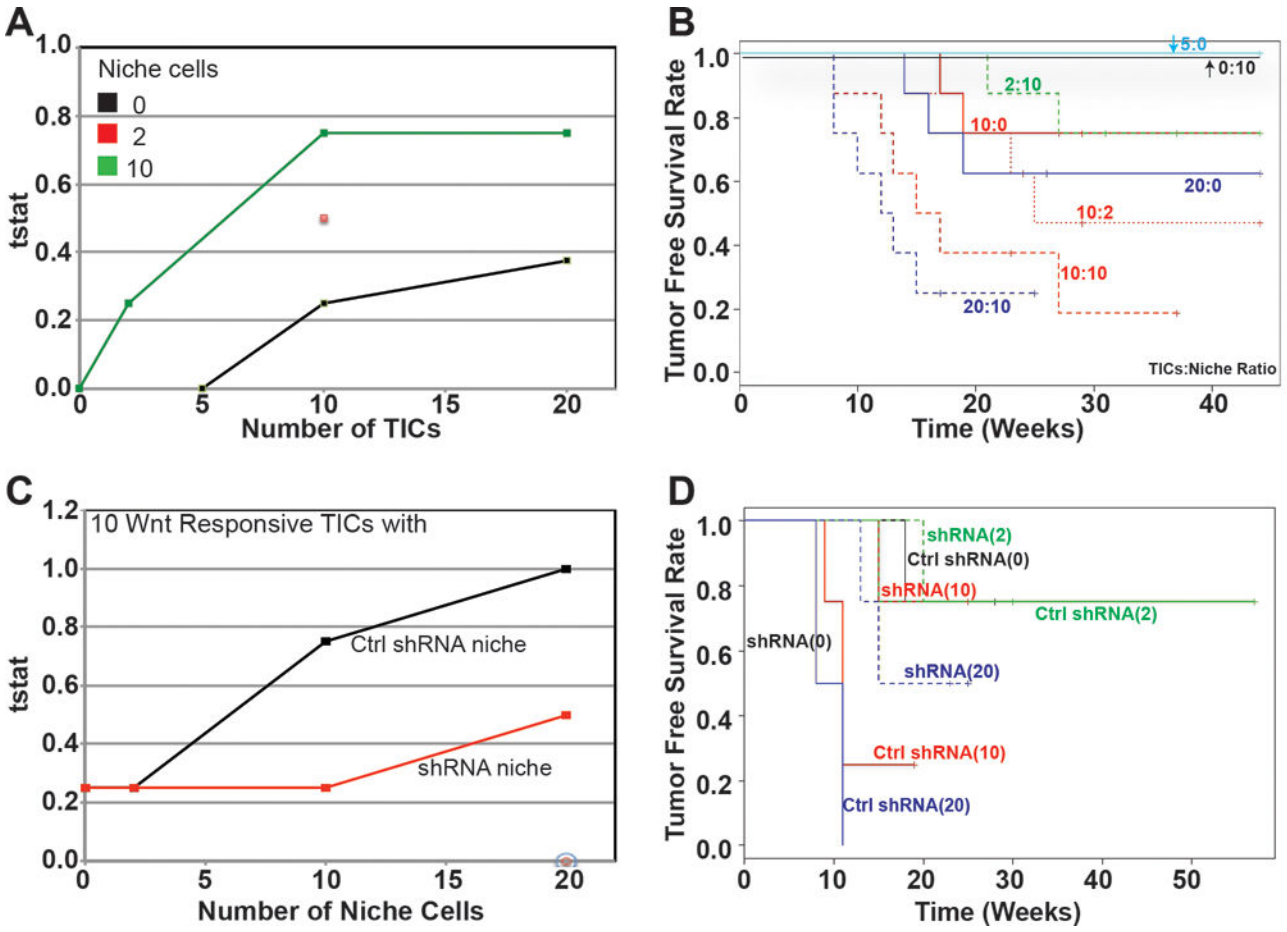

Figure 5. CD29^{H}CD24^{L} niche cells enhanced TICs tumor initiation potential shown by limiting dilution co-transplantation assays

(A) Co-transplantation of increased numbers of niche cells caused increased TIC tumor forming frequencies; (B) Niche cells reduce time to tumor formation; (C) shRNA knockdown-niche cells are associated with different tumor forming cell frequencies shown by limiting dilution co-transplantation assays; and (D) A significant difference between groups ($p<0.001$) as shown by Kaplan-Meier curves among co-transplatntation of the 10 TICs and the shRNA knockdown niche groups (cell number in parenthesis) vs that of 10 TICs and control vector groups.

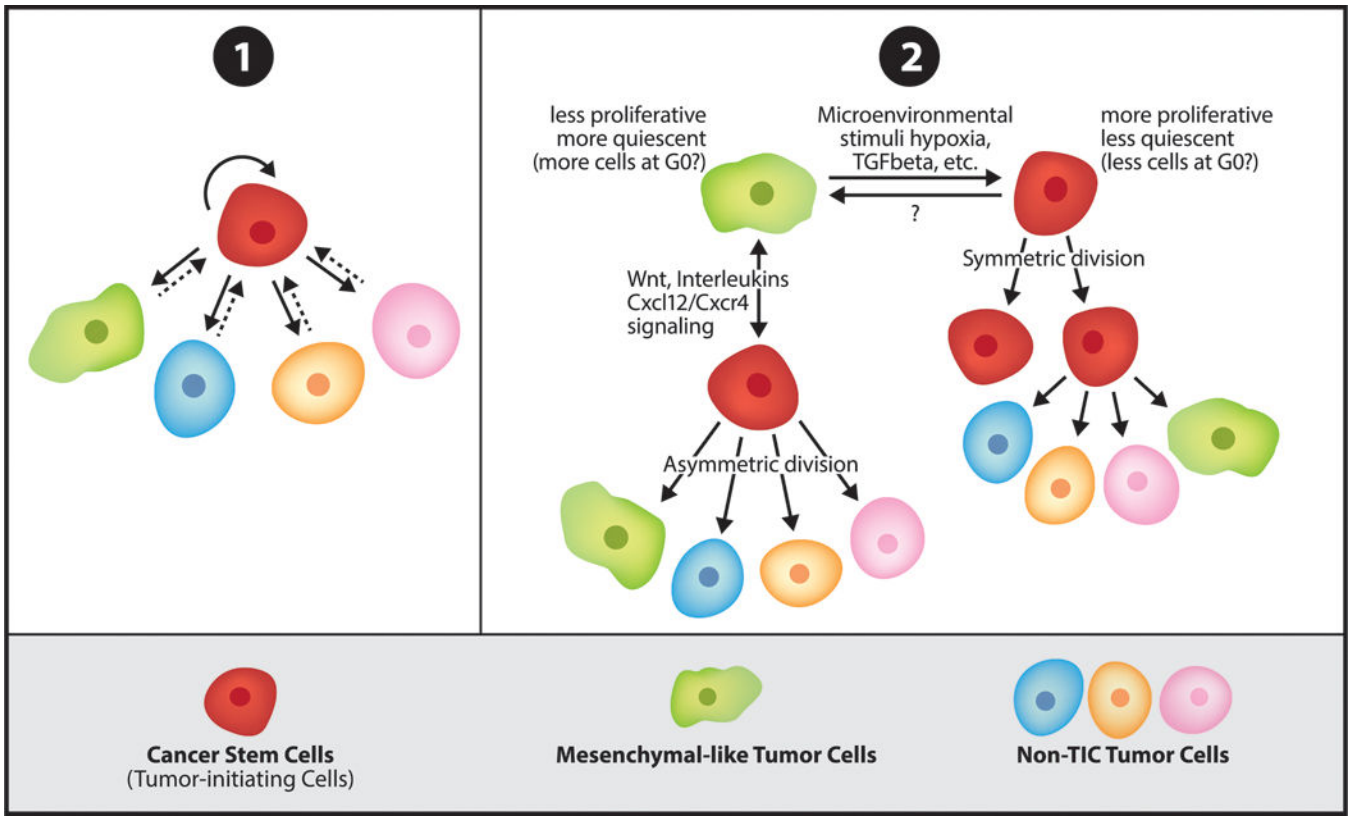

Figure 6. Tumor cell plasticity and intratumoral heterogeneity within the tumors

(1) The TIC population of cells is responsible for the generation of the vast majority of cells within a tumor. (2) The other tumor cells derived from the TICs presumably as a function of both symmetric and asymmetric division and resulting epigenetic changes due to the microenvironment and factors such as hypoxia and TGFβ may promote tumor formation especially when there are only a limited number of TICs.

Table 1

Co-transplantation of $CD29^{H}CD24^{L}$ putative niche cells with TICs

(A) Cells Co-transplanted		Efficiency of Tumor Formation (# of Tumors Formed /Transplants)	Latency of Tumor Formation (wk.) (Palpable ~ 2–3mm)
Niche Cells ($CD29^{H}CD24^{L}$)	TICs ($CD29^{H}CD24^{H}$)		
0	5	0/8	
10	2	2/8	21, 27
10	0	0/8	
0	10	2/8	17,19
2	10	4/8	14,19,23,25
10	10	6/8	8,12,13,15,17,27
0	20	3/8	14,16,19
10	20	6/8	8,8,10,12,13,15
(B) Cells Co-transplanted		**Efficiency of Tumor Formation (# of Tumors Formed /Transplants)**	**Latency of Tumor Formation (wk.) (Palpable ~ 2–3mm)**
Ctrl shRNA Transduced Niche Cells ($CD29^{H}CD24^{L}$)	**Wnt Responsive Cells (GFP +)**		
0	10	1/4	18
20	0	0/4	
2	10	1/4	15
10	10	3/4	9,11,11
20	10	4/4	8,8,11,11
Cells Co-transplanted		**Efficiency of Tumor Formation (# of Tumors Formed /Transplants)**	**Latency of Tumor Formation (wk.) (Palpable ~ 2–3mm)**
Wnt2 shRNA Transduced Niche Cells ($CD29^{H}CD24^{L}$)	**Wnt Responsive Cells (GFP +)**		
0	10	1/4	20
20	0	0/4	
2	10	1/4	20
10	10	1/4	15
20	10	2/4	13,15